

JOURNAL OF MAGNETIC RESONANCE 6, 39–54 (1972)

## Spin Echo Experiments on $^{13}\text{C}$ , $^2\text{H}$ , $^1\text{H}$ , and $^{19}\text{F}$ in Some Small Molecules in the Liquid Phase

U. HAEBERLEN, H. W. SPIESS, AND D. SCHWEITZER

*Max-Planck-Institut, Abt. Molekulare Physik 69 Heidelberg, Jahnstrasse 29, Germany*

Received August 9, 1971

The dependence on the  $\pi$  pulse repetition rate  $(2\tau)^{-1}$  of the Carr–Purcell (CP) spin echo decay constant  $R$  is studied for four nuclei in  $\text{C}_6\text{H}_6$ ,  $\text{C}_6\text{D}_6$ ,  $\text{C}_6\text{F}_6$ ,  $\text{C}_6\text{H}_{12}$ ,  $\text{C}_6\text{H}_5\text{CH}_3$ ,  $\text{CH}_3\text{I}$ ,  $\text{H}_2\text{O}$ ,  $\text{D}_2\text{O}$ , and  $\text{CS}_2$ . Both deuteron resonances, the proton resonances of  $\text{CH}_3\text{I}$ , of extremely pure  $\text{H}_2\text{O}$  and  $\text{C}_6\text{H}_6$  and the  $^{13}\text{C}$  resonance of  $\text{CS}_2$  yield straight lines when  $R$  is plotted *vs.*  $(2\tau)^2$ , i.e.,  $R$  is governed by transverse relaxation and diffusion. However, in some unexpected cases,  $T_2$  is found to be smaller than  $T_1$ . The H and F resonances of  $\text{C}_6\text{H}_6$ ,  $\text{C}_6\text{F}_6$ , and  $\text{H}_2\text{O}$  with traces of impurities do not give straight-line plots of  $R$  *vs.*  $(2\tau)^2$ . An oscillatory dependence of  $R$  on the pulse repetition rate is found for the  $^{13}\text{C}$  resonances of  $\text{C}_6\text{H}_6$  and  $\text{C}_6\text{H}_5\text{CH}_3$ . It can be shown to be due to the  $J$  coupling of the  $^{13}\text{C}$  spins to the directly bonded protons. The theory developed for exchange of chemically shifted spins can be applied and is extended for the slow exchange limit to an  $\text{AX}_3$  system in an effort to explain the results of methyl  $^{13}\text{C}$  quantitatively.

Because of the sensitivity of CP measurements on instrumental effects a detailed description is given of the measurement procedures and of the equipment of which a superconducting solenoid is an essential part. A connection between Carr–Purcell measurements, of the Gill–Meiboom version, and spin-locking experiments is pointed out.

### I. INTRODUCTION

The Carr–Purcell–Gill–Meiboom (CPGM) studies reported in this paper were motivated by  $^{13}\text{C}$  Fourier transform spectroscopy (1–4). For this field experimental  $T_2$  data of  $^{13}\text{C}$  are needed. CPGM measurements are generally believed to be very susceptible to a great variety of experimental difficulties. In order to test our apparatus, therefore, we also carried out measurements on proton, deuteron, and fluorine resonances. In some liquids our results agree with basic theoretical predictions and—when available—also with previous measurements. We take this as a confirmation that our apparatus works reliably. An essential part of our equipment is a superconducting solenoid. Its superb inherent stability reduces a great deal the difficulties encountered in earlier CPGM experiments. Some liquids, e.g., benzene, showed unexpected novel features. These will be described in Section III.

One difficulty of  $T_2$  measurements of  $^{13}\text{C}$  is connected with the experimental technique itself. Because transverse relaxation of  $^{13}\text{C}$  is often a slow process, practically the only way to measure its rate is via the CPGM technique, which, in a sense, must be used for an operational definition of  $T_2$ . Very often  $^{13}\text{C}$  nuclei are  $J$ -coupled to other nuclei with magnetic moments. In such cases the rate  $R$  of the decay of the envelope of

the CPMG echo train cannot be described by a relaxation time  $T_2$  plus, possibly, a self-diffusion term.  $R$  then depends on the pulse repetition rate  $(2\tau)^{-1}$  and three physical parameters:

- (i) the spin-spin coupling constant  $J$ ,
- (ii) the spin-lattice relaxation time  $T_{1, \text{other}}$  of the other nuclei,
- (iii) the transverse relaxation time  $T_2^0$ , the  $^{13}\text{C}$  spins would assume if  $T_{1, \text{other}}$  was infinite.

In fact, our  $^{13}\text{C}$  measurements on benzene provide a good example for the "slow exchange limit" of the theory of exchange processes studied by pulsed NMR (5-7). This theory is extended in an appendix to a four-site, unequal population case and applied to the  $^{13}\text{C}$  resonance of the methyl group in toluene.

## II. EXPERIMENTAL

### *Apparatus*

A Bruker variable frequency pulse spectrometer BK-R-306-s was used for most of the measurements. It was implemented by a (second) ND 3MD Schomandl frequency synthesizer, which was used as master oscillator for the digital pulse programmer instead of the standard 1 MHz source. This unit enabled us to vary the pulse repetition rate  $(2\tau)^{-1}$  in virtually arbitrarily small steps with quartz stability and precision. In view of the strong dependence on  $\tau$  of our results the necessity of such a fine and precise variability of  $\tau$  is obvious. The homemade NMR probes were the same as described previously (8). The temperature of the samples was monitored with a stream of nitrogen gas and measured with a thermocouple near the sample. The length of the  $\pi/2$  pulses for protons was about 1.5  $\mu\text{sec}$ , and, according to the  $\gamma$ 's, 6  $\mu\text{sec}$  for  $^{13}\text{C}$  and 10  $\mu\text{sec}$  for  $^2\text{H}$ . The tuning of the probe, which varies with temperature and which depends on the sample, was continuously checked by observing the reflected pulse power with the aid of a directional coupler. This is very convenient, especially when working with samples with long  $T_1$  and small signal-to-noise ratios. It also provides a very sensitive test for electrical breakdowns in the probe.

As already mentioned, a superconducting solenoid (Siemens SUMA 75/50/280H) proved to be an essential part of the equipment, not only because of the high field it produces ( $H_{\text{max}} = 80 \text{ kG}$ ), but also because of its excellent stability. The stability of the entire system is good enough for phase sensitive detection. This is usually not the case when a current regulated electromagnet is used. When the magnetic flux of the solenoid in the persistent mode has settled and when the probe has reached thermal equilibrium, no more drifts are detectable in the field frequency relation and in the phases. The homogeneity of the magnet is such that spin echoes at 60 MHz are about 1.2 msec wide (full width at half-height).

Since some of our proton results are rather puzzling, we made a few measurements on a completely different instrument<sup>1</sup> including NMR probes, in an effort to track down hypothetical peculiarities in our instrument. This second apparatus included an iron magnet the homogeneity of which was at least five times better than that of our solenoid.

<sup>1</sup> This instrument was made available by Bruker Physik AG, Forchheim, which help is gratefully acknowledged.

Except for trivial differences due to the different homogeneities and stabilities of the magnets the results on both instruments were the same.

#### *Adjustments, Measurement Procedure, and Checks*

Since CP experiments are apt to arise more, and no doubt justifiable, scepticism than probably any other type of NMR pulse experiment (at least when the result is not  $T_1 = T_2$ ) we give here a rather detailed description of the adjustment procedure adopted in this work.

With roughly adjusted pulses and the solenoid in its persistent mode we set the rf synthesizer exactly on resonance and, if necessary, retune the probe. All measurements reported here were made exactly on resonance. However, going out of resonance by as far as a few kHz does not change the results. The  $\pi/2$  condition for the first pulse in the CP train is adjusted by making sure that it completely destroys any  $z$  magnetization (8). Then we adjust the reference phase of the phase sensitive detector for maximum signal after the  $\pi/2$  pulse. A first rough adjustment of the  $\pi$  pulses with respect to their width and phase uses the height and symmetry of a spin echo as criteria. We then switch on the CP train and observe the first 10 or 20 echoes. They usually alternate somewhat in size. The differences usually can be reduced to a barely visible residue by additional small phase and width corrections of the  $\pi$  pulses. If not, the whole procedure is repeated.

A storage scope proves to be extremely helpful for these adjustments. Only the probe needs to be retuned on changing samples. During the measurements proper we measure the envelope of the echo train at *high*, and individual echoes at *slow* pulse repetition rates. The sweep of the scope is calibrated against the quartz crystal of the frequency synthesizer. The size of the echoes is read directly from the screen of the storage scope and immediately plotted logarithmically versus time. No systematic deviations from straight lines were found, which is noteworthy in connection with self-diffusion (see Section III).

The scatter of individual runs under identical conditions is very small, and in fact, often beyond detectability. This does not mean that we claim our measurements to be very precise but rather that systematic errors of unknown origin usually predominate over statistical ones.

From time to time we checked the sensitivity of our results with respect to pulse widths and phases by misadjusting these parameters at will. We were amazed how little these changes affected the decay constants of the echo trains. This leads us to the conclusion that *stability* is the major requirement for successful CP experiments.

As we expected trouble from the inhomogeneity of the rf field, we checked its influence in two ways: (i) We made test runs with samples much smaller than our usual ones. No difference in the decay rate of the echoes was observed. (ii) We misadjusted coarsely the width of the nominal  $\pi$  pulses. Again, the decay rates did not change drastically. This is not as surprising as it might seem at first sight, since, especially at high pulse repetition rates, the CP pulse experiment in its Gill–Meiboom version is essentially a spin-locking experiment. The crucial point is that it keeps the magnetization always parallel to the applied rf field. The fact that in a Carr–Purcell–Gill–Meiboom experiment the rf is not continuously present does not matter nor does the nutation angle of an individual pulse as long as the pulse repetition rate is high enough

to prevent the echoes from disappearing before the next pulse arrives. Therefore, in a Carr–Purcell–Gill–Meiboom experiment one measures at high pulse repetition rates  $T_{1\rho}$ , the spin-lock spin lattice relaxation time (9) rather than  $T_2$ , though in liquids the difference may be rather academic (10, 11).

### III. RESULTS AND DISCUSSION

The rate of decay of the spin echoes in a Carr–Purcell experiment on a nonviscous liquid characterized by a single transverse relaxation time  $T_2$  is given by (11)

$$R = 1/T_2 + \frac{1}{3}\gamma^2 G^2 D\tau^2. \quad [1]$$

Here  $G$  is the magnitude of the field gradient assumed to be constant over the sample, and  $D$  is the coefficient of self-diffusion. We note that, if  $G$  is *not* constant over the sample, the decay of the spin echo train is no longer exponential (12), especially when  $\tau$  is large. However, if one *defines*  $R$  as *initial* slope of the decay it is still given by Eq. [1], with  $G^2$  replaced by an appropriate average.

Thus the natural way to determine  $1/T_2$  is to measure  $R$  as a function of  $\tau$  and to plot  $R$  vs.  $\tau^2$ . A straight line should result and its intersection with the ordinate gives  $1/T_2$ . However, this procedure is usually not followed (13). Previous workers preferred to choose  $\tau$  so small that the diffusion term in Eq. [1] could be assumed to be negligible. For very long  $T_2$  as are encountered with  $^{13}\text{C}$ , this procedure can require very short  $\tau$  and the corresponding high rf power may easily heat up the sample unduly during the long pulse train. Moreover, by not checking the functional relationship between  $R$  and  $\tau$ , special features of the relaxation process may easily escape notice. The reason for not plotting  $R$  vs.  $\tau^2$  probably is that with ordinary current stabilized magnets, not trimmed for high resolution and accompanying high stability, the reproducibility of results tends to be very poor, especially if  $\tau$  is larger than the width of the echoes.

Reproducibility at all  $\tau$ 's is no problem with a superconducting coil in its persistent mode and examples of plots of  $R$  vs.  $\tau^2$  are given below. In those cases where exchange processes influence the function  $R = R(\tau)$ , we plot, according to tradition (5, 6),  $\log R$  vs.  $\log \tau^{-1}$ .

#### *Simple Cases— $R$ is Determined by $T_2$ and Diffusion*

In deuterated water (for which no data are given) and benzene (deuteron resonance at 14 MHz, Fig. 1), in  $\text{CH}_3\text{I}$  (proton resonance at 62 MHz, Fig. 2a), and in  $\text{CS}_2$  ( $^{13}\text{C}$  resonance at 62 MHz, Fig. 3)  $R$  behaves according to Eq. [1]. For deuterated samples we find, moreover,  $T_1 = T_2$  as expected from theory (11).

Indeed, the deuteron measurements were mainly intended as a test for proper operation of our apparatus. The test is, perhaps, not too meaningful because  $T_2$  of deuterons is rather short—1.5 sec in  $\text{C}_6\text{D}_6$  and 0.4 sec in  $\text{D}_2\text{O}$  at room temperature. A much more stringent test is provided by  $\text{CH}_3\text{I}$  for which we obtain  $T_1 = 11.5$  sec [see also Refs. (14, 15)] and  $T_2 = 10.6$  sec. The difference  $(1/T_2) - (1/T_1)$ , if significant at all, can be accounted for by the coupling of the protons to the fast relaxing iodine spins.

The situation becomes more complicated with  $\text{CS}_2$ , although the plot of  $R$  vs.  $\tau^2$  gives still a straight line.  $T_1$  is found to be larger than  $T_2$ ; at 20°C,  $T_1 = 39$  sec and  $T_2 = 23.4$  sec. Shoup *et al.* (16) also find  $T_2 < T_1$  at 15 MHz.

By direct measurement we found that the temperature of our  $\text{CS}_2$  sample rises considerably (up to more than 10°C) during a CP train when  $\tau$  becomes smaller than

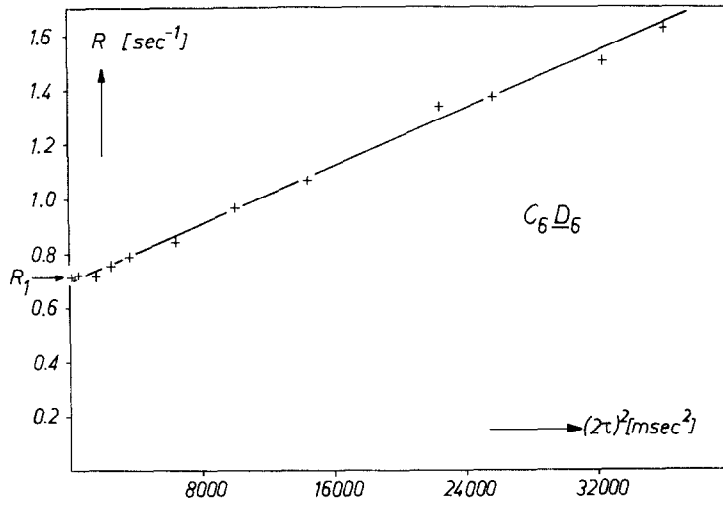


FIG. 1. CP decay rates  $R$  of the deuterium resonance of  $\text{C}_6\text{D}_6$ . The arrow indicates  $R_1 = 1/T_1$ .

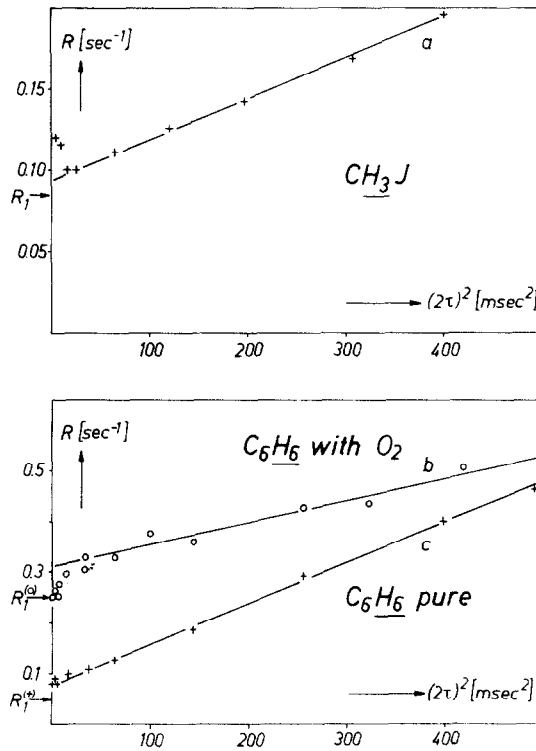


FIG. 2. CP decay rates of the proton resonances of  $\text{CH}_3\text{I}$  (a), of normal  $\text{C}_6\text{H}_6$  exposed to air (b), and of carefully degassed benzene puriss. 99.9% (CG) (Fluka, Buchs, Switzerland). The arrows indicate again the spin lattice relaxation rates.

approximately 2 msec. At room temperature the points for  $2\tau < 4$  msec deviate markedly from the straight line *towards larger values of  $R$* .<sup>2</sup>

In order to circumvent the temperature problem, we performed measurements at 221°K (Fig. 3) where  $dT_1/dT = 0$  (17). We find  $T_1 = 52.5$  sec and  $T_2 = 35$  sec. Note that the ratios  $T_2/T_1$  of our room temperature and 221°K data sets are about equal, though both  $T_2$  and  $T_1$  are considerably longer at 221°K than at room temperature. This suggests that the difference between  $T_1$  and  $T_2$  is real and not caused by instrumental

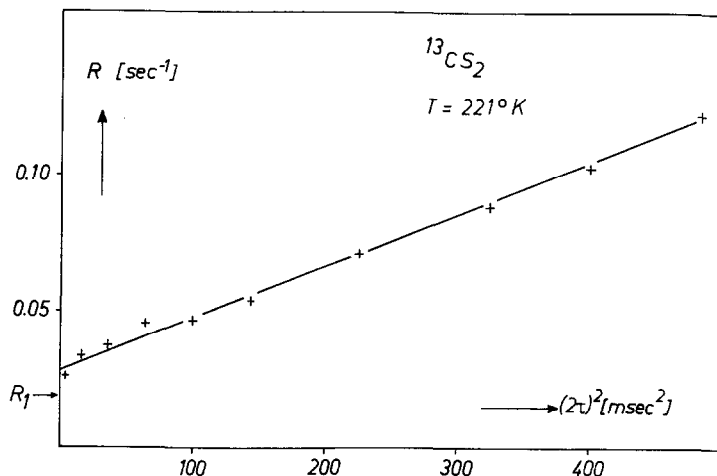


FIG. 3. Carbon-13 CP decay rates  $R$  of  $\text{CS}_2$  at 221°K. 60% enriched sample.

effects. Instrumental effects tend to reduce the apparent  $T_2/T_1$  ratios rapidly with increasing  $T_1$  (13a). The difference between  $T_1$  and  $T_2$  if real cannot be understood at present. In  $\text{CS}_2$  at least  $T_1$  is largely dominated by spin rotation and anisotropic chemical shift interactions. At 221°K and 62 MHz the two contributions are about equal and current theories (11, 18) predict for such a situation  $T_2/T_1 = 12/13$ , which is significantly larger than our experimental value. At room temperature where relaxation by spin rotation dominates,  $T_2/T_1$  should be very close to unity (18).

#### Involved Cases— $R$ Does not Obey Eq. [1]

Great efforts have been concentrated on the measurement of the proton  $T_2$  in liquid benzene. In what are probably the most careful studies so far (13a,c) the conclusion was reached that  $T_2$  equals  $T_1$ . However, no serious attempt was made to verify Eq. [1] for benzene.

In Fig. 2b a plot of the proton  $R$  vs.  $(2\tau)^2$  is given for benzene which has not been degassed. For large  $\tau$   $R$  behaves as expected, but the extrapolation does not lead to  $T_1 = T_2$ . For small  $\tau$  the measured points fall below the extrapolated straight line, and, in fact, approach  $1/T_1$ . Note that the range of decay rates is higher here than in  $\text{CH}_3\text{I}$ , therefore instrumental effects can safely be excluded as cause for the discrepancy

<sup>2</sup> A temperature rise could also have been a problem at high pulse repetition rates with the  $^{13}\text{C}$  measurements of Shoup *et al.* (16) on  $\text{CH}_3\text{I}$  and  $\text{CH}_3\text{COOCD}_3$

between this experiment and theoretical expectation. Note also if we had measured  $R$  only at small  $\tau$ , nothing peculiar would have been noticed, and we, too, would have concluded  $T_1 = T_2$  as previous workers did. The same trend as in Fig. 2b was found in a partially degassed sample of  $\text{C}_6\text{H}_6$  for which  $T_1$  at  $19^\circ\text{C}$  was as large as 15.5 sec and also for the  $^{19}\text{F}$  resonance in a pure degassed  $\text{C}_6\text{F}_6$  sample.

One set of data was collected from a sample of benzene which was not only extremely carefully degassed, but which was also, according to the manufacturer's analysis, much purer than our previous samples with respect to chemical impurities. Essentially all points from this sample fall on the straight line (Fig. 2c). However,  $T_2$  falls short of  $T_1$ , which in this case was 19 sec at  $20^\circ\text{C}$ . No explanation for this behavior can be proposed so far.

Water behaves similarly to benzene. The plots of  $R$  for distilled degassed water are straight for long  $\tau$  but do not extrapolate to  $1/T_1$ . They bend down at small  $\tau$  and approach  $1/T_1$ . Working at different  $\text{H}_0$ -homogeneities (see Section II) reveals that the experimental points start to deviate from the straight line when  $2\tau$  becomes smaller than the width of the echoes.

When the pH is varied by addition of NaOH or HCl, the plots become altogether straight and extrapolate to  $1/T_1$ . This is in accordance with the results of Meiboom (19). However, when  $\text{H}_2\text{O}$  is kept neutral by means of a buffer the plots are still straight and extrapolate to  $1/T_1$ . Extremely pure water ( $T_1 = 3.2$  sec at  $20^\circ\text{C}$ ), obtained from the Heidelberg Geophysics Laboratory, behaves like extremely pure benzene. It gives a straight plot but does not intersect the ordinate at  $1/T_1$ .

Results similar to those of protons of partially purified benzene were obtained from  $^{13}\text{C}$ . In Fig. 4,  $R$  of  $^{13}\text{C}$ , after correction for diffusion contributions, has been plotted logarithmically *vs.*  $\log(2\tau)^{-1}$ . Again  $R$  drops on reducing  $\tau$ . However, in contrast to the proton results the  $^{13}\text{C}$  results can be satisfactorily explained as follows.

Due to the  $J$  coupling with the adjacent proton the spectrum of the  $^{13}\text{C}$  resonance is split into two lines which can be labeled by the spin quantum number  $m$  of the proton. When  $m$  changes in the course of proton relaxation, the resonance of the  $^{13}\text{C}$  jumps from one line to the other. The situation is the same as for chemical exchange between two equally populated chemically shifted sites and the two cases can be treated identically as has been pointed out by Gutowsky *et al.* (7).

For the case of slow exchange between two equally populated sites with separation  $\delta\omega/2\pi$  Allerhand *et al.* (6) and Gutowsky *et al.* (7) obtain

$$R = \frac{1}{T_2^0} + k - \frac{1}{2\tau} \sin h^{-1} \left\{ \left[ \frac{\delta\omega^2}{4k^2} - 1 \right]^{-1/2} \sin \left( 2k\tau \left[ \frac{\delta\omega^2}{4k^2} - 1 \right]^{1/2} \right) \right\}, \quad [2]$$

where  $k$  is the rate constant of the exchange process assumed to be a first-order process and  $T_2^0$  is the transverse relaxation time in the absence of chemical exchange. For  $^{13}\text{C}$  in benzene  $\delta\omega$  has to be replaced by  $2\pi J$  and  $k$  by  $1/2T_{1\text{H}}$ , where  $T_{1\text{H}}$  is the proton spin lattice relaxation time.<sup>3</sup>

<sup>3</sup> Gutowsky *et al.* suggest that  $k$  be identified by  $1/T_{1\text{H}}$ . However, when spin relaxation in a spin 1/2 system is treated as a rate process, one gets in the steady state  $N_-k_{-+} = N_+k_{+-}$  and  $1/T_1 = (k_{-+} + k_{+-}) \approx 2k$  (see, e.g., C. P. Slichter, "Principles of Magnetic Resonance," Chap. 1, Harper and Row, New York, 1966.)

Since  $\delta\omega^2/4k^2 \rightarrow (2\pi J/T_{1H})^2 \gg 1$  in all of our cases we can approximate  $R$  as given by Eq. [2] safely by

$$R \approx \frac{1}{T_2^0} + k \left[ 1 - \frac{\sin(2\pi J\tau)}{2\pi J\tau} \right]. \quad [3]$$

In order to make the effect of proton relaxation on  $^{13}\text{C}$  Carr–Purcell echo trains more dramatic we added various amounts of the free radical DBNO (di-tert-butyl nitroxide) to benzene and obtained the results shown in the upper part of Fig. 4.

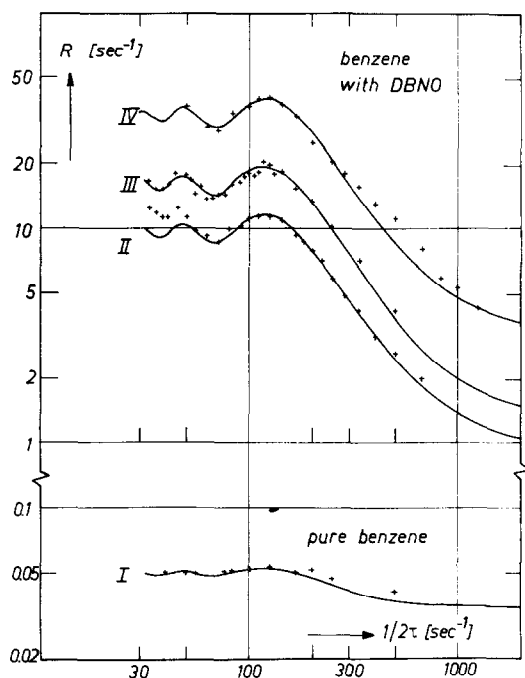


FIG. 4. Carbon-13 CP decay rates  $R$  of pure benzene (I) and of benzene doped with about 5, 10 and 20% of free radicals DBNO (II, III, IV) at room temperature. The solid curves are theoretical (Eq. [2]) with parameters shown in Table 1. The data shown for pure benzene are corrected with respect to diffusion.

The full curves are theoretical and the parameters used are compared in Table 1 with independently measured proton and  $^{13}\text{C}$  spin lattice relaxation times and with  $J$  obtained from high resolution NMR (20).

As a matter of fact,  $T_2^0$  has been set equal to  $T_{1C}$  and has not been treated as an independent parameter. From the fit obtained in Fig. 4 it is clear that our data do not contradict the assumption  $T_{1C} = T_2^0$ , but the range of uncertainty is large enough to cover the relative difference found for the nuclear relaxation times of the protons in benzene and of the  $^{13}\text{C}$  in  $\text{CS}_2$ .

A fit of our data with the high resolution NMR value of  $J$  is definitely poorer than the one finally chosen here. The cause for the discrepancy, small as it is, is not clear.



TABLE 1

PARAMETERS INSERTED INTO EQ. [2] FOR CALCULATION OF CURVES I-IV IN FIG. 4 AND INDEPENDENTLY DETERMINED COMPARABLE QUANTITIES

	Parameters for curves I-IV			Independent measurements		
	$k[\text{sec}^{-1}]$	$(T_2^0)^{-1}[\text{sec}^{-1}]$	$J[\text{Hz}]$	$(T_{1\text{H}})^{-1}[\text{sec}^{-1}]$	$(T_{1\text{C}})^{-1}[\text{sec}^{-1}]$	$J^a[\text{Hz}]$
I	0.016	0.034	168	0.05	0.034	158.7
II	8.71	0.99	168	27.0	0.99	158.7
III	14.95	1.35	168	39.0	1.35	158.7
IV	30.0	3.5	168	66.0	3.5	158.7

<sup>a</sup> See Ref. (20, p. 1023).

The agreement between directly and indirectly measured proton spin lattice relaxation times is sufficient to confirm that indeed  $k$  has to be identified with  $(2T_{1\text{H}})^{-1}$ ; in fact, for the lower concentration of free radicals and for pure benzene  $k$  is even closer to  $(3T_{1\text{H}})^{-1}$ .

*Toluene*

Only the resonance of the methyl  $^{13}\text{C}$  was studied.  $^{13}\text{C}$  enriched samples (methyl carbon, 60%) were available. Whereas benzene represents a two-site equal-population case, the  $^{13}\text{C}$  resonance of a methyl group is a four-site unequal-population case. An approximate treatment of the "slow exchange" limit is given in the Appendix.

The results of pure toluene are shown in Fig. 5a, together with two theoretical curves for which  $T_2^0$  has been set equal to  $T_{1\text{C}}$  and  $J = 126$  Hz has been taken from the literature (20). Adjustable parameters are the rates  $k_1$  of a single proton spin flip and  $k_2$  of a pairwise proton spin flip. The step height  $1/T_1(\tau \rightarrow \infty) - 1/T_1(\tau \rightarrow 0)$  determines the sum  $3k_1 + \sqrt{3}k_2$ . This can be compared with the proton spin lattice relaxation time which, in terms of  $k_1$  and  $k_2$ , is given by  $1/T_1 = 2k_1 + 4k_2$  and yields  $T_{1\text{H}} = 12$  sec. The directly measured value is  $T_{1\text{H}} = 10$  sec (21). The ratio  $k_1/k_2$  affects most strongly but still not very sensitively the transition region around  $(2\tau)^{-1} \approx J$ . All intermolecular interactions which affect the proton relaxation rate contribute to  $k_1$  as does the spin rotation interaction. According to simple relaxation theory (11) 20% of the intramolecular dipole-dipole relaxation rate are due to single and 80% to double spin flips. The value adopted for curve B,  $k_1/k_2 = 2/3$ , is in reasonable agreement with the inter- and intramolecular dipole-dipole relaxation rates of benzene measured by Green and Powles (21), and with the spin-rotation relaxation rate of the methyl protons of toluene (21).

If  $k_2$  was zero we would obtain curve A which is identical with a curve for a two-site case. In fact, the difference between phenyl ring and methyl  $^{13}\text{C}$  with respect to  $R$  is not so much a matter of populations and sites but one of possible relaxation transitions of the  $J$  coupled partners of the  $^{13}\text{C}$  spin. The partners of a methyl  $^{13}\text{C}$  can undergo  $\Delta M = \pm 2$  transitions induced by intramolecular dipole-dipole interactions whereas the proton partner of a benzene  $^{13}\text{C}$  can undergo only  $\Delta M = \pm 1$  transitions. The occurrence of  $\Delta M = \pm 2$  transitions of the methyl spins destroys to a large extent the oscillation of

$\log R$  vs.  $\log(\tau)^{-1}$  by destructive interference of two oscillations. Note that the oscillations have decayed considerably before *constructive* interference occurs.

Curve B definitely approaches the experimental points closer than does curve A, however, the discrepancies are still beyond the experimental errors. This may be due to the neglect of the difference of the rates  $R_2^0$  of the quartet and doublet components of the four "sites" (22).

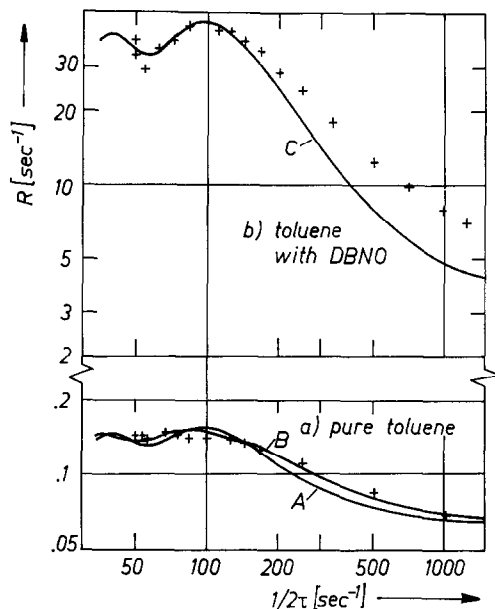


FIG. 5. Carbon-13 CP decay rates  $R$  of the methyl carbon of pure and doped toluene; 60%  $^{13}\text{C}$  enriched samples. The solid curves are theoretical;  $k_2/k_1 = 0$  for curves A and C and  $k_2/k_1 = 2/3$  for curve B. The data shown for pure toluene are corrected with respect to diffusion.

Adding free radicals, DBNO, to toluene increases  $k_1$  drastically but leaves  $k_2$  largely unaffected. Figure 5b clearly shows an oscillatory behavior of  $\log R$ . The observable maximum and minimum are consistent with  $J = 126$  Hz and jumps between neighboring sites only.

The discrepancy between experimental points and theoretical curve for  $\tau^{-1} > J$  was also observed by Shoup and VanderHart on  $^{13}\text{CH}_3\text{I}$  and  $^{13}\text{CH}_3\text{COOCD}_3$ . If, as these authors suggest,  $\Delta M = \pm 2$  transitions are taken into account, even bigger difficulties are encountered in the region of the first maximum of  $R$ .

The proton relaxation of methyl iodide is largely due to spin-rotation interaction (15), therefore  $k_1 \gg k_2$ . According to Eq. [A17], the four-site and two-site cases merge in this limit. This explains why the experimental results of Shoup and VanderHart can be satisfactorily fitted to a two-site theoretical curve.

### Cyclohexane

Cyclohexane behaves differently from all other cases studied (see Fig. 6). An exceptional behavior of cyclohexane was also observed by Allerhand and Cochran (3). They tested the SEFT technique on a variety of liquids and obtained poor results from

$\text{C}_6\text{H}_{12}$ . This becomes immediately clear with our CPGM measurements. Allerhand and Cochran take the failure of the SEFT technique as evidence for a modulation of the carbon-hydrogen coupling by the chair-chair isomerization process.

While it is tempting to assume that both their results and ours are related to the interconversion process, the mechanism is puzzling. First, the spin coupling constant changes only very little ( $\approx 4$  Hz) when a proton goes from an equatorial to an axial position; and second, the rate of the interconversion process at room temperature is very much greater (23, 24) than all other rates and frequencies which conceivably may come into play ( $\tau^{-1}$ ,  $J$ , chemical shift differences). So one should expect that cyclohexane is a case of the fast exchange limit in which no dependence of  $R$  on  $\tau^{-1}$  is predicted (6, 7).

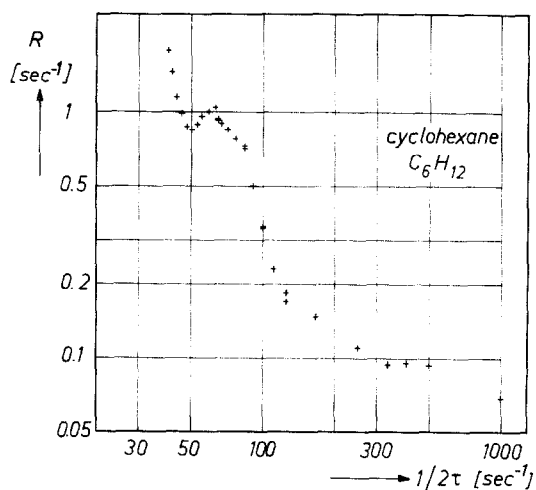


FIG. 6. Carbon-13 CP decay rates  $R$  of pure, natural  $^{13}\text{C}$  abundance cyclohexane at room temperature. The data are *not* corrected with respect to diffusion. Diffusion accounts for a small part of the general rise of the data points at small pulse repetition rates.

On the basis of comparing frequencies and rates it seems that the bump on the general rise of  $R$  has an origin similar to that of the oscillation found for benzene and toluene.

#### IV. CONCLUDING REMARKS

In  $^{13}\text{C}$  Fourier transform spectroscopy and its more sophisticated versions, DEFT and SEFT, one chooses the  $\pi$  pulse separation  $2\tau$  such that  $(2\tau)^{-1} \ll J_{\text{max}}$ . In this limit the usual assumption  $T_{2\text{C}} \approx T_{1\text{C}}$  is a poor and too optimistic guess. A good approximation which seems to be of rather general validity in organic chemistry is  $T_{2\text{C}}^{-1} \approx T_{1\text{C}}^{-1} + (2T_{1\text{H}})^{-1}$ .

By strongly irradiating the  $J$  coupled spins, i.e., protons, fluorines, etc., one may switch over from the *slow exchange* limit studied in this work to the *fast* or even *very fast* exchange limit in which  $T_{2\text{C}}$  approaches  $T_{1\text{C}}$ . The rf power requirements to reach this limit do not seem to be beyond the present state of the art.

With respect to  $T_2$  measurements of proton,  $^{19}\text{F}$  spins, etc., by the CPGM technique, we would like to point out that the large variety of cases found in this work and the *a priori* uncertainty about the functional relationship between  $R$  and  $\tau$  makes it always

imperative to *vary*  $\tau$  and to check the validity of Eq. [1]. Because of the tendency that  $T_{1\rho}$  rather than  $T_2$  is obtained by the CPGM technique when the width of the echoes exceeds the  $\pi$  pulse separation it is not sufficient to use a homogeneous magnet, unless its homogeneity is so high that application of spin echo techniques is no longer appropriate.

## APPENDIX

### *AX<sub>n</sub> System in the Limit of Slow Exchange*

The case of a coupled AX system has been treated by Gutowsky, Vold, and Wells (7). Analytic expressions were obtained for the CP decay constants  $R^{-1}$  as functions of  $\tau$ . No attempt has been made so far to obtain closed expressions for the AX<sub>n</sub> system. It is shown in this appendix that closed formulas may be derived for  $n > 1$  in the case of slow exchange. We treat an AX<sub>3</sub> system explicitly, having in mind a <sup>13</sup>CH<sub>3</sub> group. The calculation is a direct extension of Ref. (7) and notation is chosen accordingly.

The motion of the system is described by a matrix equation of the form

$$d\mathfrak{M}/dt = \mathcal{A} \cdot \mathfrak{M}, \quad [\text{A1}]$$

the general solution of which is

$$\mathfrak{M}(t) = \exp(\mathcal{A}t) \mathfrak{M}(0). \quad [\text{A2}]$$

The entries of the column vector  $\mathfrak{M}$  correspond to the transitions of the steady state absorption spectrum (7). If the initial  $\pi/2$  pulse is nonselective, we have

$$\mathfrak{M}(0) \propto \begin{pmatrix} 1 \\ 3 \\ 3 \\ 1 \end{pmatrix}. \quad [\text{A3}]$$

In the high temperature approximation a  $\pi$  pulse will only interchange states of equal weight, thus the odd and even progressions in the CP train are superposed (7).

Assuming that the site transverse relaxation rates "in the absence of exchange" are all equal ( $R_0$ ) the matrix  $\mathcal{A}$  in Eq. [A1] reads:

$$\mathcal{A} = \begin{pmatrix} (3i\Omega - R_0 - 3k_1 - 3k_2) & k_1 & k_2 & 0 \\ 3k_1 & (i\Omega - R_0 - 3k_1 - k_2) & 2k_1 & 3k_2 \\ 3k_2 & 2k_1 & (-i\Omega - R_0 - 3k_1 - k_2) & 3k_1 \\ 0 & k_2 & k_1 & (-3i\Omega - R_0 - 3k_1 - 3k_2) \end{pmatrix}. \quad [\text{A4}]$$

Here  $\Omega$  is half of the difference in frequency (in rad/sec) of the inner pair of the quartet, and  $k_1$  and  $k_2$  are the probabilities per second for flipping a given spin and spin pair, respectively. The set of differential equations describing the decay of the *proton* magnetization can also be written in terms of  $k_1$  and  $k_2$ . The result for the main decay constant is  $1/T_{1H} = 2k_1 + 4k_2$ .

The  $\mathcal{A}$  matrix as defined in [A4] is not symmetric. However, a set of equations equivalent to [A1] with symmetric  $\mathcal{A}$  can be obtained by multiplying the first and last equation of the set [A1] by  $\sqrt{3}$  and redefining

$$\mathfrak{M}(0) \propto \begin{pmatrix} \sqrt{3} \\ 3 \\ 3 \\ \sqrt{3} \end{pmatrix}. \quad [\text{A5}]$$

Hence

$\mathcal{A} =$

$$\begin{pmatrix} 3i\Omega - R_0 - 3k_1 - 3k_2 & \sqrt{3}k_1 & \sqrt{3}k_2 & 0 \\ \sqrt{3}k_1 & i\Omega - R_0 - 3k_1 - k_2 & 2k_1 & \sqrt{3}k_2 \\ \sqrt{3}k_2 & 2k_1 & -i\Omega - R_0 - 3k_1 - k_2 & \sqrt{3}k_1 \\ 0 & \sqrt{3}k_2 & \sqrt{3}k_1 & -3i\Omega - R_0 - 3k_1 - 3k_2 \end{pmatrix}. \quad [\text{A6}]$$

The echoes are observed at times  $2n\tau$  and thus it is sufficient to know  $\mathfrak{M}(2n\tau)$  for all  $n$ . As is shown in Ref. (7), the solution of Eq. [A1] may be written

$$\mathfrak{M}(2n\tau) = \mathcal{E}^n \mathfrak{M}(0) \quad [\text{A7}]$$

$$\mathcal{E} = \exp(\mathcal{A}\tau) P \exp(\mathcal{A}\tau),$$

where  $P$  describes the effect of the  $\pi$  pulses (7). From the eigenvalues of  $\mathcal{E}$ ,  $E_i$ , the CP decay constants can be obtained and are given by  $D_i = -1/2\tau \cdot \ln E_i$ . In order to calculate  $\mathcal{E}$  we have to know  $\exp(\mathcal{A}\tau)$ . This matrix can be obtained by first diagonalizing  $\mathcal{A}$  by a similarity transformation, the result of which is  $\mathcal{A}_{\text{diag}}$ , and subsequently performing the inverse transformation on the diagonal matrix  $\exp(\mathcal{A}_{\text{diag}}\tau)$  (7).

$\mathcal{A}$  can be written as

$$\mathcal{A} = -(R_0 + 3k_1 + 3k_2)\mathbb{1} + \mathcal{A}' + k', \quad [\text{A8}]$$

where  $\mathbb{1}$  is the unit matrix,

$$\mathcal{A}' = \begin{pmatrix} 3i\Omega & \sqrt{3}k_1 & \sqrt{3}k_2 & 0 \\ \sqrt{3}k_1 & i\Omega & 2k_1 & \sqrt{3}k_2 \\ \sqrt{3}k_2 & 2k_1 & -i\Omega & \sqrt{3}k_1 \\ 0 & \sqrt{3}k_2 & \sqrt{3}k_1 & -3i\Omega \end{pmatrix}, \quad \text{and} \quad k' = \begin{pmatrix} 0 & 0 & 0 & 0 \\ 0 & k_2 & 0 & 0 \\ 0 & 0 & k_2 & 0 \\ 0 & 0 & 0 & 0 \end{pmatrix}. \quad [\text{A9}]$$

In our case we must diagonalize  $\mathcal{A}' + k'$ . In the limit of slow exchange,  $k_1 \ll \Omega$ , and therefore,  $\mathcal{A}'$  is quasi-diagonal. Then all the off-diagonal elements of  $\mathcal{A}'$  can be removed to first order by three subsequent rotations, characterized by the small angles  $\varphi$ ,  $\psi$ , and  $\xi$ . Also,  $k'$  is unaffected by this transformation to first order.

The diagonalizing matrix  $\mathcal{L}$ , defined by

$$\mathcal{A}'_{\text{diag}} = \mathcal{L}^{-1} \mathcal{A}' \mathcal{L} \quad [\text{A10}]$$

and approximated to first order in the small quantities  $\sin \varphi$ ,  $\sin \psi$ , and  $\sin \xi$  is given by

$$\mathcal{L} = \begin{pmatrix} \cos \varphi \cos \xi & -\sin \xi & -\sin \varphi & 0 \\ \sin \xi & \cos \varphi \cos \psi \cos \xi & -\sin \psi & -\sin \varphi \\ \sin \varphi & \sin \psi & \cos \varphi \cos \psi \cos \xi & -\sin \xi \\ 0 & \sin \varphi & \sin \xi & \cos \varphi \cos \xi \end{pmatrix}; \quad [\text{A11}]$$

$$\mathcal{L}^{-1} = \tilde{\mathcal{L}},$$

where  $\varphi$ ,  $\psi$ , and  $\xi$  are given by

$$\begin{aligned} \sin 2\varphi &= \frac{\sqrt{3}k_2}{\sqrt{3k_2^2 - 4\Omega^2}}, & \cos 2\varphi &= \frac{2i\Omega}{\sqrt{3k_2^2 - 4\Omega^2}}; \\ \sin 2\psi &= \frac{2k_1}{\sqrt{4k_1^2 - \Omega^2}}, & \cos 2\psi &= \frac{i\Omega}{\sqrt{4k_1^2 - \Omega^2}}; \\ \sin 2\xi &= \frac{\sqrt{3}k_1}{\sqrt{3k_1^2 - \Omega^2}}, & \cos 2\xi &= \frac{i\Omega}{\sqrt{3k_1^2 - \Omega^2}}. \end{aligned} \quad [\text{A12}]$$

We can now calculate  $\mathcal{E}$ , where further simplification arises from the fact that the eigenvalues of  $\mathcal{A}$  are equal to the diagonal elements of  $\mathcal{A}$  in the original basis to first order.

$$\mathcal{E} = \exp(2k_2 \tau) \begin{pmatrix} 0 & a & d & x \\ a & h & y & f \\ d & y & g & c \\ x & f & c & 0 \end{pmatrix}$$

with

$$\begin{aligned} a &= \sin 2\varphi [\exp(4i\Omega\tau) - \cosh 2k_2 \tau], & c &= \sin 2\varphi [-\exp(-4i\Omega\tau) + \cosh 2k_2 \tau], \\ d &= \sin 2\xi [\exp(2i\Omega\tau) - \cosh 2k_2 \tau], & f &= \sin 2\xi [-\exp(-2i\Omega\tau) + \cosh 2k_2 \tau], \\ g &= \sin 2\psi [-\exp(-2i\Omega\tau) + 1] \exp 2k_2 \tau, & h &= \sin 2\psi [\exp(2i\Omega\tau) - 1] \exp 2k_2 \tau, \\ x &= \cos^4 \varphi \cos^4 \xi \exp(-2k_2 \tau) + \sin^2 2\varphi (\cosh 4i\Omega\tau - \frac{1}{2} \cosh 2k_2 \tau) \\ &\quad + \sin^2 2\xi (\cosh 2i\Omega\tau - \frac{1}{2} \cosh 2k_2 \tau), \\ y &= \cos^4 \varphi \cos^4 \psi \cos^4 \xi \exp(2k_2 \tau) + \sin^2 2\varphi (\cosh 4i\Omega\tau - \frac{1}{2} \cosh 2k_2 \tau) \\ &\quad + \sin^2 2\psi (\cosh 2i\Omega\tau - \frac{1}{2}) \exp(2k_2 \tau) + \sin^2 2\xi (\cosh 2i\Omega\tau - \frac{1}{2} \cosh 2k_2 \tau). \end{aligned} \quad [\text{A13}]$$

If not only  $k_2 \ll \Omega$  but also  $k_2 \tau \ll 1$ , the eigenvalues of  $\mathcal{E}$  can be approximated by  $1 + G$  and  $-1 + H$  with  $|G|, |H| \ll 1$ . Neglecting terms of third and fourth order in  $H$  and  $G$  the secular equation can be reduced to a quadratic equation for  $G$  and  $H$ , and we obtain for the eigenvalues:

$$E_{1,2} = 1 + \frac{B}{\sqrt{3}} \pm \sqrt{(F+B)^2 + \left(\frac{B}{\sqrt{3}} + 2k_2 \tau\right)^2}$$

and

$$E_{3,4} = -1 + \frac{B}{\sqrt{3}} \pm \sqrt{(F-B)^2 + \left(\frac{B}{\sqrt{3}} - 2k_2 \tau\right)^2},$$

[A14]

where

$$B = 1/2(d + f) = \sin 2\xi \sin h(i2\Omega\tau)$$

and

$$F = 1/2(a + c) = \sin 2\varphi \sin h(i4\Omega\tau);$$

note that  $B$  and  $F$  are always real.

The signal  $S(2n\tau)$ , with phase sensitive detection, is given by (7)

$$S(2n\tau) = \mathbb{1} \cdot \mathfrak{M}(2n\tau). \quad [\text{A15}]$$

In order to obtain  $S(2n\tau)$  as a sum of exponentials with different decay constants and amplitudes, each component of the column vector  $\mathfrak{M}(2n\tau)$  has to be written as a sum of these exponentials. This can be done in an analogous way as was described above for obtaining  $\exp(\mathcal{A}\tau)$ .

Thus if  $Q$  diagonalizes  $\mathcal{E}$  so that

$$\mathcal{E}_{\text{diag}} = Q^{-1} \mathcal{E} Q, \quad [\text{A16}]$$

the—diagonal—matrix of the decay constants is

$$\mathcal{D} = -(1/2\tau) \ln \mathcal{E}_{\text{diag}}. \quad [\text{A17}]$$

Combining Eqs. [A17] through [A15] and [A7] we obtain for the signal

$$S(2n\tau) = \mathbb{1} \cdot Q \cdot \exp(-2n\tau\mathcal{D}) Q^{-1} \mathfrak{M}(0). \quad [\text{A18}]$$

$\mathcal{E}$  is a complex symmetric matrix. Clearly we can also calculate the signal from  $\mathcal{E}^2$ , thus considering the even echoes only ( $n$  even).  $\mathcal{E}^2$  is real symmetric to first order in the small quantities  $B$ ,  $F$ , and  $k_2$ :

$$\mathcal{E}^2 = \begin{pmatrix} 1 - 4k_2\tau & 2B & 2F & 0 \\ 2B & 1 + 4k_2\tau & \frac{4}{\sqrt{3}}B & 2F \\ 2F & \frac{4}{\sqrt{3}}B & 1 + 4k_2\tau & 2B \\ 0 & 2F & 2B & 1 - 4k_2\tau \end{pmatrix}. \quad [\text{A19}]$$

The matrix  $\mathcal{E}^2$  can now be diagonalized by a real orthogonal transformation.<sup>4</sup> It can be determined explicitly, since the eigenvalues of  $\mathcal{E}$  and hence  $\mathcal{E}^2$  are known.

$$\begin{aligned} S(t) \propto & A_1 \exp \left\{ -t \left[ R_0 + 3k_1 + 2k_2 - \frac{1}{2\tau} \left( \frac{B}{\sqrt{3}} + \sqrt{(F+B)^2 + \left( \frac{B}{\sqrt{3}} + 2k_2\tau \right)^2} \right) \right] \right\} \\ & + A_2 \exp \left\{ -t \left[ R_0 + 3k_1 + 2k_2 - \frac{1}{2\tau} \left( \frac{B}{\sqrt{3}} - \sqrt{(F+B)^2 + \left( \frac{B}{\sqrt{3}} + 2k_2\tau \right)^2} \right) \right] \right\} \end{aligned} \quad [\text{A20}]$$

with

$$\begin{aligned} A_1 &= [-2a_2/(a_1 - a_2)](1 + a_1)(\sqrt{3} + 3a_1), \\ A_2 &= [2a_1/(a_1 - a_2)](1 + a_2)(\sqrt{3} + 3a_2), \end{aligned}$$

<sup>4</sup> The reason for calculating the eigenvalues of  $\mathcal{E}$  rather than those of  $\mathcal{E}^2$  directly is the fact that the secular equation of  $\mathcal{E}^2$  cannot be reduced to quadratic equations by the approximation  $1 + G$  or  $-1 + H$ .

and

$$a_1 = \frac{1}{F+B} \left( \frac{B}{\sqrt{3}} + 2k_2 \tau \pm \sqrt{(F+B)^2 + \left( \frac{B}{\sqrt{3}} + 2k_2 \tau \right)^2} \right).$$

It is seen that in this approximation the signal contains contributions with two different time constants, where the relative amplitudes are functions of the pulse separation  $2\tau$ .

For  $\tau \rightarrow 0$ ,  $A_2$  vanishes and only one time constant is observed. If either  $k_2 \ll k_1$  or vice versa, the signal is typically dominated by one of the contributions [A20]. For the case  $k_1 \approx k_2$  the two amplitude factors are comparable only for  $\tau$  such that the two time constants are both relatively close to their mean value for long  $\tau$ :  $R_\infty = R_0 + 3k_1 + \sqrt{3}k_2$ . In this case the observed decay constant may be calculated as a weighted arithmetic mean of the two time constants.

#### ACKNOWLEDGMENTS

We would like to thank Prof. K. H. Hausser for his interest in this work. Our special thanks are due to H. Zimmermann for quick and careful sample preparation.

#### REFERENCES

1. R. R. ERNST AND W. A. ANDERSON, *Rev. Sci. Instr.* **37**, 93 (1966).
2. E. D. BECKER, J. A. FERRETTI, AND T. C. FARRAR, *J. Amer. Chem. Soc.* **91**, 7784 (1969).
3. A. ALLERHAND AND D. W. COCHRAN, *J. Amer. Chem. Soc.* **92**, 4482 (1970).
4. J. S. WAUGH, *J. Mol. Spectrosc.* **35**, 298 (1970).
5. Z. LUZ AND S. MEIBOOM, *J. Chem. Phys.* **39**, 366 (1963).
6. A. ALLERHAND AND H. S. GUTOWSKY, *J. Chem. Phys.* **42**, 1587 (1965).
7. H. S. GUTOWSKY, R. L. VOLD, AND E. J. WELLS, *J. Chem. Phys.* **43**, 4107 (1965).
8. H. JÄCKLE, U. HAEBERLEN, AND D. SCHWEITZER, *J. Magn. Resonance* **4**, 198 (1971).
9. A. G. REDFIELD, *Phys. Rev.* **98**, 1787 (1955).
10. G. P. JONES, *Phys. Rev.* **148**, 332 (1966).
11. A. ABRAGAM, "The Principles of Nuclear Magnetism," Oxford University Press, London, 1961.
12. K. A. VALIEV, *Sov. Phys. Usp.* **7**, 835 (1966).
13. (a) K. H. WEISS, Ph.D. thesis, Karl-Marx-Universität, Leipzig, 1966.  
 (b) K. H. WEISS, Proc. XIV Coll. Amp., 981, North-Holland Publ. Co., Amsterdam, 1966.  
 (c) W. DIETRICH, Ph.D. thesis, Technische Hochschule, Aachen 1968.  
 (d) W. DIETRICH AND R. KOSFELD, *Z. Naturforsch. A* **24**, 1209 (1969).  
 (e) R. HAUSSER AND F. NOACK, *Z. Naturforsch. A* **19**, 1521 (1964).  
 (f) U. HAEBERLEN, R. HAUSSER, F. NOACK, AND G. MAIER, *Phys. Lett.* **12**, 306 (1964).
14. M. D. ZEIDLER, *Ber. Bunsenges. Phys. Chem.* **69**, 659 (1965).
15. K. T. GILLEN, M. SCHWARTZ, AND J. H. NOGGLE, *Mol. Phys.* **20**, 899 (1971).
16. R. R. SHOUP AND D. L. VANDERHART, *J. Amer. Chem. Soc.* **93**, 2053 (1971).
17. H. SPIESS, D. SCHWEITZER, U. HAEBERLEN, AND K. H. HAUSSER, *J. Magn. Resonance*, **5**, 101 (1971).
18. P. S. HUBBARD, *Phys. Rev.* **131**, 1155 (1963).
19. S. MEIBOOM, *J. Chem. Phys.* **34**, 375 (1961).
20. J. W. EMSLEY, J. FEENEY, AND L. H. SUTCLIFFE, "High Resolution NMR Spectroscopy," Vol. 2, Pergamon Press, Oxford, 1966.
21. D. K. GREEN AND J. G. POWLES, *Proc. Phys. Soc.* **85**, 87 (1965).
22. W. BUCHNER AND B. EMMERICH, *J. Magn. Resonance* **4**, 90 (1971).
23. A. ALLERHAND, F. M. CHEN, AND H. S. GUTOWSKY, *J. Chem. Phys.* **42**, 3040 (1965).
24. F. A. L. ANET AND A. J. R. BOURNE, *J. Amer. Chem. Soc.* **89**, 760 (1967).